Proton migration mechanism for operational instabilities in organic field-effect transistors

A. Sharma,[1,][*] S. G. J. Mathijssen,[1,2] E. C. P. Smits,[2] M. Kemerink,[1] D. M. de Leeuw,[2] and P. A. Bobbert[1]

[1]*Eindhoven University of Technology, P.O. Box 513, 5600 MB Eindhoven, The Netherlands*
[2]*Philips Research Laboratories Eindhoven, High Tech Campus 4, 5656 AE, Eindhoven, The Netherlands*

Organic field-effect transistors exhibit operational instabilities involving a shift of the threshold gate voltage when a gate bias is applied. For a constant gate bias the threshold voltage shifts toward the applied gate bias voltage, an effect known as the bias-stress effect. Here, we report on a detailed experimental and theoretical study of operational instabilities in *p*-type transistors with silicon-dioxide gate dielectric both for a constant as well as for a dynamic gate bias. We associate the instabilities with a reversible reaction in the organic semiconductor in which holes are converted into protons in the presence of water and a reversible migration of these protons into the gate dielectric. We show how redistribution of charge between holes in the semiconductor and protons in the gate dielectric can consistently explain the experimental observations. Furthermore, we show how a shorter period of application of a gate bias leads to a faster backward shift of the threshold voltage when the gate bias is removed. The proposed mechanism is consistent with the observed acceleration of the bias-stress effect with increasing humidity, increasing temperature, and increasing energy of the highest molecular orbital of the organic semiconductor.

I. INTRODUCTION

Organic field-effect transistors (OFETs) are the basic building blocks of low-cost contactless identification transponders, electronic barcodes, and pixel engines of flexible active matrix displays.[1,2] However, a severe limitation of the commercial introduction of OFETs is their operational stability. During operation, the current modulation by the gate bias decreases over time, leading to a gradual malfunctioning. This electrical instability is manifested as a shift of the threshold voltage—the gate bias voltage at which a transistor switches on—with time.[3,4] This undesirable effect is usually referred to as the "bias-stress effect." The identification of its origin is of paramount importance for the development of commercially viable OFETs.

The bias-stress effect has been extensively studied in *p*-type organic transistors with silicon dioxide, SiO_2, as the gate dielectric.[5–14] SiO_2 is chosen to prevent effects of ionic movements, which are known to occur in organic gate dielectrics.[15] Nevertheless, transistors with SiO_2 as gate dielectric suffer from the bias-stress effect. The effect is usually studied by applying a constant stressing gate bias, interrupted by short time intervals in which the transfer curve—the source-drain current as a function of gate bias for a small applied source-drain voltage—is measured. The main observation in these measurements is that the whole transfer curve shifts in the direction of the constant stressing gate bias.

The threshold-voltage shift as a function of time is customarily fitted with a stretched-exponential function, as is done in similar studies on the bias-stress effect in amorphous-silicon FETs.[16] Despite the success of such a fit, there is no agreement on the microscopic mechanism behind the effect. Several mechanisms have been suggested as an explanation, such as (i) trapping of mobile carriers in the bulk of the semiconductor,[17] (ii) trapping in disordered areas of the semiconductor,[7] (iii) trapping in regions in between crystalline grains of the semiconductor,[18] (iv) trapping in

states at the semiconductor/dielectric interface,[8] and (v) pairing of mobile carriers to bipolarons in the semiconductor.[5,19] Two other important observations are that the effect is influenced by humidity[13,20,21] and that the effect is thermally activated, with an activation energy of about 0.6 eV, apparently independent of the organic semiconductor used.[11]

Recently, we proposed a mechanism for the bias-stress effect in *p*-type field-effect transistors with SiO_2 gate dielectric that is based on production of protons from holes and water in the accumulation layer of the semiconductor and the subsequent migration of these protons into the gate dielectric.[14] We showed that this mechanism can quantitatively explain the measured dependence of the threshold-voltage shift on time and that this dependence can indeed be accurately fitted with a stretched-exponential function. We concluded that to a good approximation the drift contribution to the motion of the protons can be neglected so that this motion is governed by diffusion. In this approximation, the time scale of the bias-stress effect is determined by a characteristic time that depends only on the diffusion coefficient and the ratio between the proton density in the oxide at the interface with the semiconductor and the hole density in the accumulation layer of the semiconductor.[14]

A unique aspect of this mechanism is that not only the amount of protons stored in the dielectric is important but also their specific density profile. As a consequence, unlike other mechanisms, this mechanism predicts the occurrence of memory effects related to the biasing history of the transistor. Specific predictions about anomalous nonmonotonic current transients derived from the model for the case of a dynamic biasing scheme were indeed experimentally verified.[22]

One of the other interesting aspects of the bias-stress effect is that it is reversible: on applying a zero gate bias after stressing, the threshold voltage shifts back toward its original value, an effect usually referred to as "recovery." While the bias-stress effect has been thoroughly investigated, recovery has received little attention. It has been established that the

dynamics of the threshold-voltage shift for recovery is different from that for stress[11] but an explanation for this observation is still lacking. In the present paper, we present a detailed study of recovery. In particular, we investigate the effect of the extent of stressing on the recovery dynamics. We find that the recovery rate strongly depends on the extent of stressing: when the transistor has been stressed to the extent that the threshold voltage has been shifted almost completely to the stressing gate bias, the time scale for recovery is much longer than when the transistor has only partially been stressed.

The purpose of the present paper is to discuss the proton migration mechanism introduced in Refs. 14 and 22 in detail and to show how the mechanism can explain the experimental observations on recovery. The paper is built up as follows. In Sec. II, we present measurements of the bias-stress effect for a *p*-type OFET and discuss the main experimental features of the effect. In Sec. III, we introduce the proton migration mechanism and discuss its experimental and theoretical basis. In Sec. IV, we discuss the modeling of the proton migration mechanism and its application to the bias-stress effect. In Sec. V, we discuss the application of the proton migration mechanism to the case of a nonconstant bias stress, for which anomalous nonmonotonic current transients are obtained. In Sec. VI, we demonstrate how the proton migration mechanism can explain measurements on stress-recovery cycles with different extents of stressing. In Sec. VII, we discuss the influence of the energy of the highest occupied molecular orbital (HOMO) of the semiconductor on the dynamics of the bias-stress effect. Finally, Sec. VIII contains a summary and the conclusions, as well as a discussion of the results.

II. BIAS-STRESS EFFECT: EXPERIMENTAL

We investigated the bias-stress effect for a *p*-type OFET fabricated using heavily doped *p*-type Si wafers as the common gate electrode with a 200 nm thermally oxidized SiO_2 layer as the gate dielectric. Using conventional photolithography, gold source and drain electrodes were defined in a bottom-contact device configuration with a channel width (W) and length (L) of 2500 μm and 10 μm, respectively. A 10-nm-thick layer of titanium was used as an adhesion layer for the gold on SiO_2. The SiO_2 layer was treated with the primer hexamethyldisilazane (HMDS) prior to semiconductor deposition in order to passivate its surface. Polytriarylamine (PTAA) films were spun from a 1% toluene solution at 2000 rpm for 20 s, resulting in a film thickness of 80 nm. The electrical characterization was carried out using an HP 4155C semiconductor parameter analyzer under conditioned ambient atmosphere at a temperature of 30 °C. All measurements reported in the present paper have been performed on this transistor.

Figure 1(a) shows the development in time of the transfer curves of the transistor, undergoing bias stress with a constant gate voltage $V_{G0} = -20$ V for a total time of 100 h $\approx 4 \times 10^5$ s. The transfer curves were measured by interrupting the stress for brief periods of time, during which a source-drain voltage of $V_{SD} = -3$ V was applied and the gate
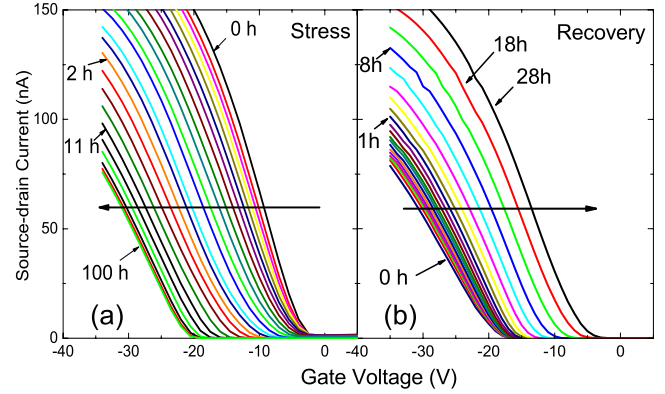

FIG. 1. (Color online) (a) Transfer curves of the investigated *p*-type transistor in ambient atmosphere at a temperature of 30 °C for different stressing times, indicated in hours (h). The gate bias voltage during stressing was $V_{G0} = -20$ V. (b) Transfer curves of the same transistor undergoing recovery with grounded electrodes for different recovery times after 28 h of stressing. The source-drain voltage while measuring the transfer curves was $V_{SD} = -3$ V. The horizontal arrows shows the shifts of the transfer curves with time.

voltage was swept. As is clearly observed, the main effect of the bias stress is a shift of the transfer curves in the direction of V_{G0}. In the course of time, the threshold voltage V_{th} (defined here as the intercept of the extrapolated linear part of the transfer curve with the voltage axis) shifts all the way down to V_{G0}. The symbols in Fig. 2(a) show the threshold-voltage shift $\Delta V_{th}(t) = V_{th}^0 - V_{th}(t)$ as a function of time t. Here, V_{th}^0 is the threshold voltage shift at the start of the experiment, which is close to zero. In studies of the bias-stress effect it has become customary to describe the shift $\Delta V_{th}(t)$ with a stretched-exponential function,[6,11,16] $\Delta V_{th}(t) = V_0(1 - \exp[-(t/\tau)^\beta])$, where the prefactor V_0 is close to $|V_{G0}|$, τ is a relaxation time, and $0 < \beta < 1$ an exponent. As can be seen in Fig. 2(a) this function (dashed curve) yields a very good fit. The fit parameters are $V_0 = 19$ V, $\tau = 10^4$ s, and $\beta = 0.43$.

Many studies have shown that humidity has a profound influence on the bias-stress effect. Under vacuum conditions, with practically no water present on the SiO_2 interface, the bias-stress effect is greatly slowed down.[6,11,20,21] This is evident from the relaxation time of $\tau = 2 \times 10^6$ s obtained from the bias-stress measurements on a similar PTAA transistor in vacuum,[11] which is more than two orders of magnitude larger than the above value in ambient. Furthermore, pretreatment of the SiO_2 with hydrophobic HMDS or octadecyltrichlorosilane is is known to decelerate the effect.[9,13] Use of a hydrophobic organic gate dielectric practically eliminates the effect[21] while coverage of the SiO_2 with a layer that is impenetrable to water does the same.[10] These observations indicate that the threshold-voltage shift in organic transistors is related to residual water.

Another aspect of the bias-stress effect is that the dynamics of the threshold voltage shift during stressing does not depend on the source-drain bias. This was demonstrated in a study in which the source-drain current of a device undergoing stress was monitored under constant source-drain bias and then compared to the case when the gate bias was kept
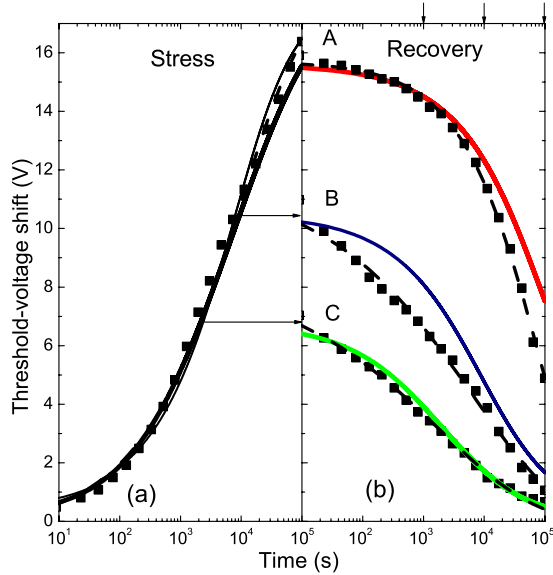
FIG. 2. (Color online) Symbols: experimentally obtained threshold-voltage shift $\Delta V_{th}(t)$ as a function of time t. (a) During stress with a gate voltage of $V_{G0}=-20$ V. (b) During recovery after three different stressing periods: 10^5 s [A, obtained from Fig. 1(b)], 10^4 s (b), and 2×10^3 s (c). The dashed lines in both (a) and (b) correspond to stretched-exponential fits. The thick lines correspond to the results of the proton migration mechanism. The thin line in (a) corresponds to a fit with also drift taken into account. The fit parameters are $D=1.6 \times 10^{-19}$ cm^2/s and $\alpha=2.2$ nm^{-1}. The times at which the proton density profiles are plotted in Fig. 5 during recovery are indicated at the upper axis in (b).

constant but the source-drain bias was switched off from time to time during the stressing period. It was found that switching off the source-drain bias during stressing had no impact on the source-drain current, which was identical to that obtained with a constant source-drain bias.[11]

The dynamics of the bias-stress effect has been measured at various temperatures.[11] It was found that for transistors with SiO$_2$ as gate dielectric and PTAA as the semiconductor the relaxation time τ decreases exponentially with increasing temperature with an activation energy of about 0.6 eV. Interestingly OFETs of other organic semiconducting polymers such as poly-3-hexylthiophene (P3HT), poly-thienylene-vinylene (PTV), and poly-dioctyl-fluorene-co-bithiophene (F8T2) showed under identical conditions thermally activated behavior with the same activation energy of 0.6 eV.[11] The independence of the activation energy on the semiconductor indicates that the bias-stress effect in transistors with SiO$_2$ gate dielectric has a common origin. It should be noted that although the activation energy for different semiconductors is the same, the value of the relaxation time is different for each of the semiconductors. We will discuss the role of the semiconductor, and in particular the energy of its HOMO, in the bias-stress effect in Sec. VII.

Recovery of the original state of the transistor can be established by applying a zero bias to the gate electrode for an extended period of time.[8,11] In this period, the transfer curve gradually shifts back to the transfer curve before stressing, as shown in Fig. 1(b), where the transistor is re-

covering after 28 h $\approx 10^5$ s of stressing. It has been found that the dynamics of V_{th} for recovery can also be fitted with a stretched-exponential function but that the parameters are different than for stress.[11] The symbols in Fig. 2(b) labeled by A represent the threshold-voltage shift as a function of time for the transfer curves in Fig. 1(b). The shift can be fitted very well with the function $\Delta V_{th}(t)=V_1 \exp[-(t/\tau)^\beta]$, with the fit parameters $\tau=7.7 \times 10^4$ s, $\beta=0.58$, and $V_1=15.7$ V. The symbols in Fig. 2(b) labeled by B and C have been obtained by starting the recovery after 10^4 and 2×10^3 s of stressing, respectively. For these recovery curves we obtain stretched-exponential fits with $\tau=6.5 \times 10^3$ s, $\beta=0.3$, and $V_1=11.7$ V (B), and $\tau=2 \times 10^3$ s, $\beta=0.28$, and $V_1=8.4$ V (C). We will extensively discuss these different recovery experiments in Sec. VI.

III. PROTON MIGRATION MECHANISM FOR THE BIAS-STRESS EFFECT

A strong indication that the bias-stress effect is not caused by trapping of charges in the organic semiconductor but by processes occurring on the SiO$_2$ surface comes from scanning Kelvin-probe microscopy measurements of the potential on a structure similar to the OFET investigated in the present paper but without deposition of the organic semiconductor.[13] With application of a drain bias (and a grounded source and gate) a time evolution of the potential profile at the SiO$_2$ surface was measured. The dynamics of this evolution was found to be determined by the amount of water on the SiO$_2$, which could be regulated by treatment with HMDS.[13] The time evolution of the potential profile on this structure shows that charges can move around reversibly on the SiO$_2$ surface even in absence of a semiconductor. Surprisingly, the time evolution was found to occur on equal time scales for both positive and negative polarity of the drain bias.[13] Since carriers with different polarities should have different transport characteristics, this observation implies that the dynamics of the potential profile is in both cases governed by one type of charge carrier.

Surface-conductivity measurements on SiO$_2$ performed in the 1960s and repeated a decade ago have revealed an ionic nature of the conductivity and it was suggested that protons (H$^+$) that are electrolytically produced from physisorbed water are the charge carriers.[23–25] It was shown that protons can be produced electrolytically from water on the SiO$_2$ surface by replacing water in the ambient by heavy water (D$_2$O) and detecting deuterium gas (D$_2$) after performing surface-conductivity measurements.[23] Therefore, we suggest that in the above experiments protons are responsible for the time evolution of the potential profiles. Because of the presence of silanol groups (SiOH) protons will be present on the SiO$_2$ surface because of the reaction SiOH$\rightleftharpoons$SiO$^-$+H$^+$, creating an acidic environment. On applying a positive bias at the drain electrode, oxidation of water occurs at this electrode, producing excess protons in the reaction $2H_2O \rightarrow 2H^+ + 2e^- + O_2(g)$. The motion of protons away from the drain electrode toward the source electrode gives rise to a positive potential profile. On the other hand, when applying a

negative bias, the reaction $2H^+ + 2e^- \rightarrow H_2(g)$ occurs at the drain electrode, leading to a deficit of protons. This results in a motion of protons toward the drain electrode, giving rise to a negative potential profile. Since under the application of both negative and positive bias it is the motion of protons that determines the potential profiles, the evolution of these profiles occurs on the same time scale.

Since organic semiconductors are permeable to water, water molecules can also reach the SiO_2 surface in the presence of an organic semiconductor. We therefore propose that in a *p*-type OFET under bias stress the electrolytic production of protons now takes place at the interface between the semiconductor and the SiO_2, where the whole accumulation layer in the semiconductor acts as a positive electrode. In this electrolytic reaction, holes in the semiconductor are converted into protons. Calculations within the framework of density-functional theory have shown that water at the Si-SiO_2 interface can undergo oxidation to produce protons in the presence of holes.[26] Although we do not know of equivalent studies for the interface between an organic semiconductor and SiO_2, it is natural to assume that the same reaction will take place. Regarding the above discussion, it is then also natural to assume that protons can be converted back into holes along with production of H_2.

The reversible motion of protons in SiO_2 has been demonstrated by memory effects occurring in $Si/SiO_2/Si$ devices, where protons move through the SiO_2 from one Si layer to the other.[27,28] Protons in SiO_2 bind to the oxygen atoms and their motion occurs by hopping from one oxygen atom to another. The mobility of protons in amorphous SiO_2 has been studied by directly sensing charge displacements, indicating hopping transport of protons with hopping lengths well beyond first-neighbor oxygen distances.[29] In a theoretical study, Godet and Pasquarello[30] showed that protons usually bind to bridging O atoms in Si-O rings that become threefold coordinated with O-H^+ bond lengths of about 1 Å. The hopping mechanism involves a transient complex, in which a proton is shared by two O atoms of different rings. The formation of the intermediate O-H^+-O complex, in which the proton forms two bonds, favors the ensuing breaking of the first O-H^+ bond, after which the proton is completely transferred from one oxygen atom to the other. Long-range diffusion of protons in SiO_2 is pictured by these authors as a percolative motion in which protons move from one oxygen atom to another through an energy barrier that depends on the distance between the two oxygen atoms. Godet and Pasquarello used molecular dynamics to generate a large-size structure of amorphous SiO_2. They assigned barrier energies for hopping of protons depending on the interoxygen distances. According to their calculations, the size of the percolation cluster approaches infinity when all the sites separated by an energy barrier less than 0.5 eV are connected.[30] This activation energy of about 0.5 eV for long-range diffusion of protons is close to the 0.6 eV activation energy found in bias-stress experiments on different organic semiconductors.[11] This strongly suggests that proton motion in the SiO_2 determines the dynamics of the bias-stress effect.

Based on these experimental and theoretical results we propose the following scenario. (i) In the presence of water, holes in the organic semiconductor, indicated below by OS^+, can be converted into protons in the electrolytic reaction
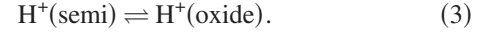
$$2H_2O + 4OS^+ \rightarrow 4H^+ + O_2(g) + 4OS, \qquad (1)$$
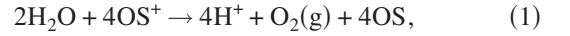
where OS refers to electrically neutral sites in the organic semiconductor. (ii) Protons can be converted back into holes in the reaction

$$2H^+ + 2OS \rightarrow 2OS^+ + H_2(g). \qquad (2)$$
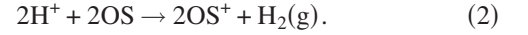
(iii) Protons in the accumulation layer of the semiconductor are in equilibrium with protons in the oxide at the interface with the semiconductor

$$H^+(\text{semi}) \rightleftharpoons H^+(\text{oxide}). \qquad (3)$$

(iv) Protons in the oxide at the interface can diffuse into the bulk of the oxide.

We note that reactions Eqs. (1) and (2) will establish an equilibrium between holes and protons in the accumulation layer. This essentially implies the reversibility of the bias-stress effect, as we will see further on. It is reasonable to assume that the dynamics of the reactions Eqs. (1)–(3) is much faster than the diffusion of protons into the bulk of the oxide. This leads to the conclusion that the dynamics of the bias-stress effect is governed primarily by the motion of protons in the oxide and not by the specific details of the reactions. Under this assumption, there will be an equilibrium between the surface density $[OS^+]$ of holes in the semiconductor and the volume density $[H^+]$ of protons in the oxide at the interface with the semiconductor, leading to the linear relation

$$[H^+] = \alpha[OS^+], \qquad (4)$$

where the parameter α is a proportionality constant, which is determined by the reaction constants. We treat α as a parameter in what follows. We note that protons in the semiconductor in the presence of water probably occur in a hydrated form (H_3O^+ or more complex coordination) but this is not central to our analysis.

IV. MODEL FOR THE PROTON MIGRATION MECHANISM: APPLICATION TO THE BIAS-STRESS EFFECT

The proposed proton migration mechanism can be made quantitative in the following way. Under the assumption that the protons do not penetrate deep into the oxide, we can write down the following charge-balance equation while stressing the OFET with a constant gate bias V_{G0}

$$\int_0^\infty p(x,t)dx + h_0(t) = c_0 \equiv \frac{CV_{G0}}{e}, \qquad (5)$$

where $p(x,t)$ is the time-dependent volume density of protons in the oxide at a distance x from the interface with the semiconductor, $h_0(t)$ is the time-dependent surface density of holes in the accumulation layer of the semiconductor, C is the capacitance of the oxide per unit area, and e is the elementary charge. In principle, diffusion as well as drift of protons in the oxide occurs. In the present derivation we will neglect drift and only take diffusion of protons into account.

Clearly, in the initial stage after the application of a gate bias there will be a large density gradient—perpendicular to the interface with the semiconductor—of protons in the oxide, such that diffusion automatically dominates over drift. The advantage of neglecting proton drift is that a clear picture of the mechanism arises and that the modeling is considerably simplified. We can then write the equation of motion for protons in the oxide as

$$\frac{\partial}{\partial t} p(x,t) = D \frac{\partial^2}{\partial x^2} p(x,t) \qquad (6)$$

with D the diffusion coefficient. This equation can be solved using the Green's function for the one-dimensional diffusion equation

$$p(x,t) = \int_0^t \int_{-\infty}^{\infty} \frac{\exp\left[-\frac{(x-x')^2}{2D(t-t')}\right] s(x',t')}{\sqrt{4\pi D(t-t')}} dx' dt', \quad (7)$$

where $s(x,t)$ stands for the source term, which is equal to the proton flux into the oxide from the accumulation layer. This source term can be obtained by differentiating Eq. (5) with respect to time and using Eq. (6)

$$s(x,t) = -2D \left. \frac{\partial p(x,t)}{\partial x} \right|_{x=0} \delta(x) = -2 \frac{dh_0(t)}{dt} \delta(x), \qquad (8)$$

where the factor 2 is related to the fact that we consider a diffusion problem in a half-space $x \geq 0$. Using the equilibrium condition $p(0,t) = \alpha h_0(t)$ and the above expression for the source term, we can calculate the proton density in the oxide at the interface as

$$p(0,t) = \int_0^t \frac{1}{\sqrt{4\pi D(t-t')}} \left[-\frac{2}{\alpha} \frac{dp(0,t')}{dt'} \right] dt'. \qquad (9)$$

On applying partial integration and replacing $p(0,t)$ with $\alpha h_0(t)$, we obtain the following equation for the hole density in the accumulation layer

$$h_0(t) = \frac{1}{2} \int_0^t \frac{t_0^{1/2}}{(t-t')^{3/2}} [h_0(t') - h_0(t)] dt' - \left(\frac{t_0}{t}\right)^{1/2} [h_0(t) - c_0], \qquad (10)$$

where the characteristic time t_0 is given by

$$t_0 \equiv \frac{1}{\pi \alpha^2 D}. \qquad (11)$$

We note that, unlike the relaxation time τ in the stretched-exponential fits to the threshold-voltage shifts discussed in Sec. II, this characteristic time is related to physical parameters.

Equation (10) can be solved for $h_0(t)$ by iterative numerical techniques. The threshold voltage is finally obtained as

$$V_{th}(t) = \frac{e}{C} [c_0 - h_0(t)]. \qquad (12)$$

The application of the model to the threshold-voltage dynamics during stressing discussed in Sec. I leads to the thick

full line in Fig. 2(a) for the case that only proton diffusion in the oxide is taken into account. For this case the dynamics of the threshold-voltage shift is described by a universal curve with t_0 as the only parameter. This fact is in agreement with the experimental observation that the dynamics of the bias-stress effect is virtually independent of the value of the applied gate voltage.[11] For the present case, we are able to obtain a good fit up to $t \approx 10^4$ s and extract $t_0 = 4.2 \times 10^3$ s.

The deviation from predictions of the diffusion model observed in Fig. 2(a) for longer times should be attributed to proton drift in the oxide. In order to take into account drift we must solve the full drift-diffusion equation for the motion of the protons. In order to do so, we need to estimate the diffusion constant and α individually. The drift component of the proton flux into the oxide can be written as $J_{drift}(t) = \mu p(0,t) E(0,t)$, where μ is the mobility of the protons and $E(0,t)$ is the electric field at the interface. On expressing $p(0,t)$ and $E(0,t)$ in terms of V_{G0} and $V_{th}(t)$, we get

$$J_{drift}(t) = \mu \alpha \frac{C[V_{G0} - V_{th}(t)]^2}{e L_{ox}}, \qquad (13)$$

where L_{ox} is the thickness of the oxide layer. In our model, the diffusive component of the flux is given by

$$J_{diff}(t) = -D \left. \frac{\partial}{\partial x} p(x,t) \right|_{x=0} = -\frac{d}{dt} h_0(t) = \frac{C}{e} \frac{d}{dt} V_{th}(t). \qquad (14)$$

Deviations from our model predictions occur when the drift component becomes comparable to the diffusive component. Assuming that this happens from $t = t_{dev}$ onwards, we obtain by equating Eqs. (13) and (14) at $t = t_{dev}$

$$\mu \alpha = \frac{L_{ox}}{(V_{G0} - V_{th}(t_{dev}))^2} \frac{d}{dt} V_{th}(t)|_{t=t_{dev}}. \qquad (15)$$

Using Einstein's relation, $D/\mu = k_B T/e$, Eq. (15), and the definition of t_0, Eq. (11), we find

$$\alpha = \frac{e}{k_B T} \frac{[V_{G0} - V_{th}(t_{dev})]^2}{\pi t_0 L_{ox} \frac{d}{dt} V_{th}(t)|_{t=t_{dev}}}, \qquad (16)$$

$$D = \left(\frac{k_B T}{e}\right)^2 \frac{\pi t_0 L_{ox}^2}{[V_{G0} - V_{th}(t_{dev})]^4} \left[\frac{d}{dt} V_{th}(t)|_{t=t_{dev}}\right]^2. \qquad (17)$$

By taking $t_{dev} \approx 10^4$ s and the experimentally determined $V_{th}(t=t_{dev})$ and $\frac{d}{dt} V_{th}(t)|_{t=t_{dev}}$, we obtain $\alpha \approx 2$ nm^{-1} and $D \approx 10^{-19}$ cm^2/s. We are not aware of any measurements of the diffusion coefficient of protons in our gate dielectric consisting of dry amorphous thermally grown SiO$_2$ but the value we find is very close to the diffusion coefficient for protons in Si$_3$N$_4$.[31]

We also directly numerically solved the drift-diffusion equation for protons in the oxide

$$\frac{\partial}{\partial t} p(x,t) = \mu p(x,t) E(x,t) - D \frac{\partial}{\partial x} p(x,t). \qquad (18)$$

The threshold voltage can be calculated using

$$V_{\text{th}}(t) = \frac{e}{\epsilon} \int_0^{L_{\text{ox}}} (L_{\text{ox}} - x) p(x,t) dx, \tag{19}$$

where ϵ is the relative dielectric constant of the oxide. The electric field at any point in the oxide can be obtained using Poisson's equation

$$E(x,t) = E(0,t) + \frac{e}{\epsilon} \int_0^{L_{\text{ox}}} p(x,t) dx,$$

$$= \frac{V_{\text{G0}} - V_{\text{th}}(t)}{L_{\text{ox}}} + \frac{e}{\epsilon} \int_0^{L_{\text{ox}}} p(x,t) dx. \tag{20}$$

We normalize the distance into the oxide x, the proton density $p(x,t)$, and the electric field $E(x,t)$ in the oxide with respect to L_{ox}, $p(0,0) \equiv \alpha h_0(t=0)$, and $E(0,0) \equiv V_{\text{G0}}/L_{\text{ox}}$, respectively. We normalize time t with respect to $L_{\text{ox}}^2/\mu V_{\text{G0}}$. Under the assumption that protons do not reach the gate electrode during the stressing period, the drift-diffusion equation along with Poisson's equation can be cast in the following form:

$$F(\hat{x},\hat{t}) = \int_{\hat{x}}^1 \hat{p}(\hat{x},\hat{t}) d\hat{x}, \tag{21}$$

$$\frac{\partial}{\partial \hat{t}} F(\hat{x},\hat{t}) = \hat{p}(\hat{x},\hat{t}) \hat{E}(\hat{x},\hat{t}) - \gamma \frac{\partial}{\partial \hat{x}} \hat{p}(\hat{x},\hat{t}), \tag{22}$$

$$\hat{E}(\hat{x},\hat{t}) = 1 - \alpha L_{\text{ox}} F(\hat{x},\hat{t}) + \alpha L_{\text{ox}} \int_0^1 \hat{x} \hat{p}(\hat{x},\hat{t}) d\hat{x}, \tag{23}$$

$$\hat{p}(0,\hat{t}) = 1 - \alpha L_{\text{ox}} \int_0^1 (1-\hat{x}) \hat{p}(\hat{x},\hat{t}) d\hat{x}, \tag{24}$$

where $\gamma = k_{\text{B}} T / e V_{\text{G0}}$. In the equations above, symbols with hats represent normalized quantities. These equations can be solved numerically by advancing time in small steps to obtain $p(0,t)$. We obtain the hole density in the channel by using Eq. (4). The threshold-voltage $V_{\text{th}}(t)$ is obtained from Eq. (12).

As shown by the thin line in Fig. 2, an excellent fit to the experimentally determined time dependence of the threshold voltage is obtained when the drift-diffusion problem is solved with $D = 1.6 \times 10^{-19}$ cm²/s and $\alpha = 2.2$ nm⁻¹. For these values of D and α, we show the proton density profile in the gate oxide for different times in Fig. 3(a). The penetration depth of the protons into the oxide is about 30 nm at the end of stressing in Fig. 1(a) ($t = 100$ h $\approx 4 \times 10^5$ s). This is much smaller than the oxide thickness of 200 nm and hence consistent with our assumption that the protons do not penetrate deep into the oxide. The results displayed in Fig. 2(a) show that the diffusive flux of protons into the oxide dominates over the drift flux of protons till $t \approx 10^4$ s. We show in Fig. 3(b) the electric field profile in the oxide for different times. Since most of the proton charge stays close to the interface between the organic semiconductor and the oxide, the electric field varies strongly with distance near the
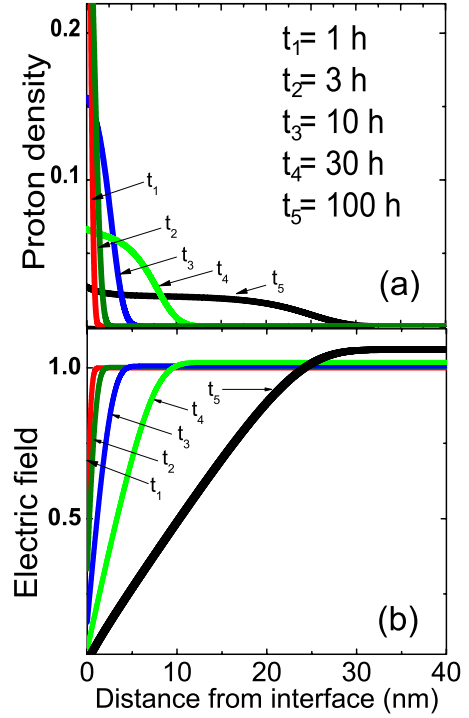

FIG. 3. (Color online) (a) Proton density profile $p(x,t)/p(0,0)$ and (b) electric field profile $E(x,t)/E(0,0)$ in the oxide at different times after the start of stressing, for a numerical solution of the drift-diffusion problem related to the proton migration mechanism.

interface, whereas there is practically no change in its value far from the interface.

V. ANOMALOUS CURRENT TRANSIENTS

The unique aspect of the proton migration mechanism, in comparison to other proposed mechanisms for the bias-stress effect, is that it is not based on trapping of charges in or very near the accumulation layer, but on a build-up of charges, the protons, in the bulk of the oxide at a distance of the accumulation layer. This means that the state of the transistor is not only determined by the total number or protons in the oxide but also by their particular density profile. In the previous section we have seen that in an ordinary bias-stress experiment with a constant stressing gate voltage the shift of the threshold voltage is monotonic and that the proton density profile decays monotonically into the bulk of the oxide. With the application of a dynamic gate bias, however, it is possible to create a nonmonotonic proton density profile, leading to a nonmonotonic time dependence of the threshold voltage. The observation of such anomalous nonmonotonic behavior is an excellent way to validate the proton migration mechanism. Indeed, we recently observed such anomalous behavior.[22] Here, we provide the quantitative description of this behavior in the light of the proton-diffusion model discussed in the previous section.

We have investigated a dynamic gate biasing scheme in which the transistor is first stressed with a strongly negative gate voltage V_{G0} and then, after time $t = t_{\text{sw}}$, stressed with a less negative gate voltage V_{G1}, which is chosen such that the
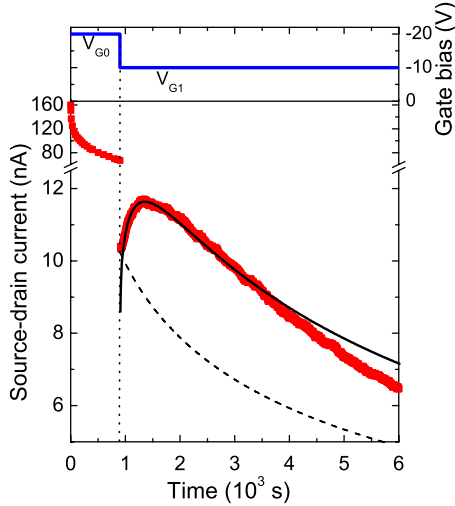
FIG. 4. (Color online) Upper panel: dynamic switching scheme of the gate bias voltage V_G. Lower panel: experimental source-drain current I_{SD} vs time t for a source-drain voltage $V_{SD}=-3$ V (thick red line) and model prediction using the same value of t_0 as obtained in Sec. IV (thin black line). The calculated I_{SD} has been shifted vertically by -2 nA, such that the experimental and theoretical maximum coincide. The vertical dotted line indicates the switching of the gate bias from V_{G0} to V_{G1}. The dashed line indicates the decreasing current as expected for other proposed mechanisms for the bias-stress effect.

transistor remains in accumulation throughout the stressing period. During the stressing, a constant small source-drain voltage V_{SD} is applied, leading to a source-drain current I_{SD} that is measured. According to the proton-diffusion model a large amount of protons should diffuse into the dielectric in the period of stressing with the strongly negative gate voltage V_{G0}, a part of which should diffuse back to the semiconductor and get reconverted into holes during stressing with the less negative voltage V_{G1}. This should lead to a nonmonotonic current, in which the current after switching from V_{G0} to V_{G1} first increases and then continues to decrease.[22] The measured source-drain current for such a dynamic biasing scheme exactly shows the predicted nonmonotonic temporal response to the switched gate bias; see Fig. 4. We remark that, unlike in the ordinary bias-stress experiment in Sec. II, we measured the source-drain current as a function of time instead of interrupting the stressing to measure a transfer curve. The reason is the relatively short time scale at which the anomalous effect occurs, which prohibits the interruption procedure.

The occurrence of anomalous current transients shows that the transistor has a memory of its "biasing history." By using a dynamic gate bias we have thus in a way probed the proton density profile in the oxide and demonstrated that the state of the transistor is indeed not only determined by the total number of protons in the oxide but also by their density profile. This demonstration is fully in line with the prediction of the proton migration mechanism.

In principle, one can construct a specific model based on competition between trapping and detrapping of mobile carriers in the accumulation layer that will give rise to similar transients on switching the gate bias. On applying such

model to the bias-stress effect under constant gate bias, it would predict a steady-state situation in which there is a balance between trapping and detrapping. However, such model would predict a saturation of the threshold voltage, which is in contrast to the observation that the threshold voltage shifts all the way to the applied gate voltage under constant stress.

The scenario explaining the anomalous transient currents can be made quantitative in the following way. The dynamic gate voltage applied to the gate electrode can be written as the sum of two step functions: $V_G(t) = V_{G0}\theta(t) - (V_{G0}-V_{G1})\theta(t-t_{sw})$, where $\theta(t)$ is the unit step function. The experiments on the anomalous current transients are conducted on a time scale where the motion of protons in the oxide is primarily dominated by their diffusion (see the discussion in the previous section). By virtue of the linearity of the diffusion equation, the solution for the surface density of holes $h(t)$ can therefore be obtained as the linear combination

$$h(t) = h_0(t) - \left(1 - \frac{V_{G1}}{V_{G0}}\right)h_0(t-t_{sw}), \quad (t > t_{sw}), \quad (25)$$

where $h_0(t)$ is the solution for the bias-stress effect described above. The threshold voltage is obtained as

$$V_{th}(t) = \frac{e}{C}[c - h(t)], \quad (t > t_{sw}), \quad (26)$$

with $c \equiv CV_{G1}/e$.

In Fig. 4 we have used the same value $t_0 = 4.2 \times 10^3$ s as found in the previous section in the comparison of the experimentally determined source-drain current I_{SD} (thick red curve) to our model result (black curve). The initial gate bias is $V_{G0}=-20$ V, which is switched to $V_{G1}=-10$ V at $t_{sw}=900$ s. We used the transfer curves shown in Fig. 1(a) to translate our predictions for $V_{th}(t)$ to predictions for $I_{SD}(t)$. This procedure inevitably introduces some errors. For example, we note that in Fig. 1(a) the slope of the transfer curves in the linear regime decreases with time, meaning that the mobility of the holes decreases. We attribute this to scattering of holes by the Coulomb fields of the protons in the oxide. This scattering will depend both on the number of protons and their penetration depth in the oxide. This means that the transfer curves are not only determined by V_{th}, leading to a slight error in our approach. Deviations from our model can also be expected when the difference between V_G and $V_{th}(t)$ becomes close to $V_{SD}=-3$ V. Both issues could have an influence on a possible offset in the current. We found that with a small downward shift of 2 nA the maximum of the theoretical curve is the same as that of the measured curve in Fig. 4. The time t_{max} at which the maximum occurs is accurately predicted without making any adjustments. In Ref. 22 we showed that the predicted t_{max} also accurately agrees with the measured value when the gate voltage V_{G1} after switching or the time of switching t_{sw} is varied. We consider this agreement, obtained without introducing any other parameter, as very strong evidence for the

proton migration mechanism. The dashed line in Fig. 4 sketches the continuing decrease of the current predicted by other models for the bias-stress effect.

VI. RECOVERY

In the present section, we focus our attention on recovery, i.e., the phenomenon that under application of a zero gate bias the transfer curve of a transistor that has suffered from bias stress shifts back to the transfer curve before the bias stress. Concomitantly, the threshold voltage shifts back to its original value. The study of recovery has received little attention in literature. It has been found that the dynamics of the threshold-voltage shift for recovery is different from that for stress[11] but an explanation for this finding has been lacking up till now. A systematic study of recovery and its dynamics is important for a better understanding of instabilities occurring in OFETs.

The different recovery experiments labeled by A, B, and C in Fig. 1(b) discussed in Sec. II have been performed in order to investigate if the extent of stressing has an influence on the dynamics of the recovery. The results clearly indicate that this is the case. The fits to a stretched-exponential function yield values for the relaxation time τ of 7.7×10^4 s (A, stressing for 10^5 s), 6.5×10^3 s (B, stressing for 10^4 s), and 2×10^3 s (C, stressing for 2×10^3 s), while the relaxation time for stress is $\tau = 10^4$ s; see Sec. II. The conclusion is that the dynamics for recovery is different from that for stress and that the relaxation times decrease with decreasing stressing time. We checked that during each stressing period the curve in Fig. 2(a) is followed, which means that the dynamics during stress remains unchanged.

The observation that the dynamics of recovery is influenced by the extent of stressing can be explained within the proton migration mechanism as follows. At the end of the stressing period, there is a density profile of protons extending into the oxide. During recovery, when the gate bias is zero, the density of holes in the accumulation layer vanishes. Because of the equilibrium condition Eq. (4) the density of protons at the interface between oxide and semiconductor also vanishes. This leads to a backdiffusion of protons from the oxide toward the semiconductor. Protons reaching the semiconductor will be converted into holes, which are carried away to the source and drain electrodes. The consequence of this is that the further away protons have diffused into the oxide during stressing, the longer it will take for these protons to diffuse back to the semiconductor. Since the depth of penetration of protons into the oxide depends on the extent of stressing, this rationalizes the observation that the time scale for recovery decreases with decreasing stressing period.

In order to describe the recovery dynamics quantitatively, we numerically solved the time-dependent proton-diffusion problem for all three stress-recovery cycles A–C. We note that, as in the previous section, we take into account only the diffusion contribution to the motion of the protons. Assuming that the device is being stressed for a total time t_{stress} before grounding the gate electrode we can write the gate voltage as a function of time in the following way:

$$V_G(t) = V_{G0}\theta(t) - V_{G0}\theta(t - t_{\text{stress}}). \tag{27}$$

In this expression, the first term can be interpreted as uninterrupted stressing of the transistor with the gate voltage V_{G0}. The contribution of this term to the proton density at the interface can be calculated by taking into account a positive source term that is injecting protons in the oxide, in the same way as in Sec. IV. The second term ensures that at $t = t_{\text{stress}}$ the gate bias becomes zero such that for $t > t_{\text{stress}}$ the hole density in the channel goes to zero. The contribution of this term to the proton density at the interface can be calculated by taking into account a negative source term corresponding to extraction of protons out of the oxide. We can therefore write for the proton density at the interface

$$\tilde{p}(0,t) = \int_0^t \frac{1}{\sqrt{4\pi D(t - t')}}[s(t') - s_{\text{rec}}(t')\theta(t - t_{\text{stress}})]dt', \tag{28}$$

where $s(t) = -(2/\alpha)dp(0,t)/dt$ and $p(0,t)$ is the density of protons at the interface for the case that the transistor is under continuous stress with the gate voltage V_{G0}. $s_{\text{rec}}(t)$ represents the source term that accounts for the second term in Eq. (27). For $t > t_{\text{stress}}$, $\tilde{p}(0,t) \equiv 0$ and therefore we can write

$$\int_0^t \frac{1}{\sqrt{4\pi D(t - t')}}s(t')dt' = \int_{t_{\text{stress}}}^t \frac{1}{\sqrt{4\pi D(t - t')}}s_{\text{rec}}(t')dt'. \tag{29}$$

Writing $t = t_{\text{stress}} + \tilde{t}$ and using Eq. (9), we can write the above equation as

$$\int_{t_{\text{stress}}}^{t_{\text{stress}}+\tilde{t}} \frac{1}{\sqrt{4\pi D(t_{\text{stress}} + \tilde{t} - t')}}s_{\text{rec}}(t')dt' = p(0, t_{\text{stress}} + \tilde{t}). \tag{30}$$

Using Eq. (4), we can write $p(0,t) = \alpha h_0(t)$, where $h_0(t)$ is the corresponding hole density in the channel for the case that the transistor is under constant stress with the gate voltage V_{G0}. Writing $s_{\text{rec}}(t) = 2r(t)/\sqrt{t}$ in the equation above, we can derive the following equation for $r(t)$:

$$r(t) = \frac{2}{\pi}h_0(t_{\text{stress}} + t) - \frac{1}{\pi}h_0(t_{\text{stress}})$$
$$+ \frac{2}{\pi}\int_0^t \sin^{-1}\left(\frac{2t'}{t} - 1\right)\frac{dr(t')}{dt'}dt'. \tag{31}$$

This equation can be solved for $r(t)$ using iterative numerical techniques. The threshold voltage during recovery can then be calculated as

$$V_{\text{th}}(t) = \frac{e}{C}\left[c_0 - h_0(t_{\text{stress}} + t) - \int_0^t \frac{r(t')}{\sqrt{t - t'}}dt'\right]. \tag{32}$$

The results for the recovery curves A–C are given by the thick lines in Fig. 2(b), using exactly the same value t_0 as found in Sec. IV. The agreement with the measured data is surprisingly good. Apparently, the proton migration mechanism captures the dynamics of the threshold voltage for tress as well as recovery.
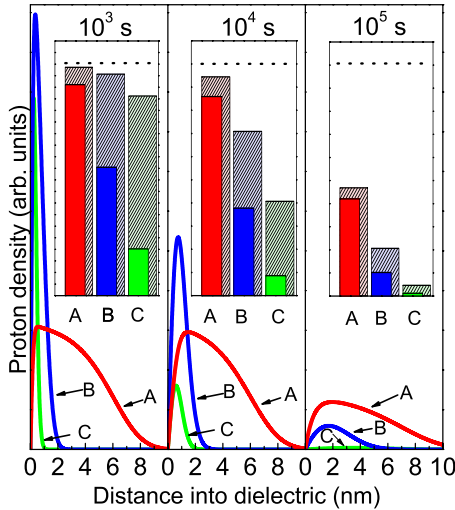
FIG. 5. (Color online) Modeled proton density profiles in the oxide during recovery after a recovery time of 10^3, 10^4, and 10^5 s (left to right). A, B, and C refer to the same stressing periods as in Fig. 2(b). Inset: bar diagrams representing the total charge (filled bars) in the oxide calculated from the model and the total charge normalized to that at the start of recovery (hatched bars). The dotted line represents the initial normalized charge at the start of recovery.

In Fig. 5 we show the proton density profiles in the oxide with proceeding recovery, calculated with the parameters $D = 1.6 \times 10^{-19}$ cm^2 s^{-1} and $\alpha = 2.2$ nm^{-1} found in Sec. IV, for three different times after the start of recovery, indicated at the upper axis in Fig. 2(b): 10^3, 10^4, and 10^5 s. The profiles labeled by A, B, and C correspond to the same stressing periods as in Fig. 2(b). We clearly see that with a shorter stressing period the protons are removed much quicker from the oxide during recovery than with a longer stressing period. To emphasize this point further, we indicate the total proton charge contained in the oxide by filled bars in the insets of Fig. 5. The hatched bars indicate the total proton charge normalized to the total amount of charge just before recovery, making clear that the *relative* recovery rate is faster in the case of a shorter stressing period. If the recovery dynamics would not depend on the stressing period, the normalized total proton charge would be the same for the situations A–C.

VII. INFLUENCE OF THE HOMO ENERGY ON THE BIAS-STRESS EFFECT

Since the production of protons occurs by oxidation of water by the organic semiconductor according to the reaction Eq. (1), there should be a relation between the speed at which the bias-stress effect occurs and the energy of the highest occupied molecular orbital, E_{HOMO}. Our model predicts that an increase in E_{HOMO} should facilitate the electrolytic production of protons from holes since an increase in E_{HOMO} makes the positively charged oxidized state of the organic semiconductor (OS$^+$) less stable. This should result in an increase of α in Eq. (4) and the speed at which the threshold-voltage shift occurs. Therefore, we considered the relaxation times τ in stretched-exponential fits to bias-stress
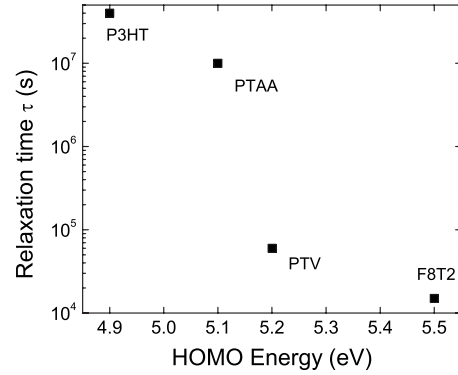

FIG. 6. Relaxation times τ obtained from measurements under identical conditions of the bias-stress effect of OFETs (Ref. 11) as a function of the energy of the highest occupied molecular orbital for four different polymeric semiconductors: P3HT, PTAA, PTV, and poly-dioctyl-fluorene-co-bithiophene (F8T2).

measurements of OFETs based on different organic semiconductors[11] and compared those to E_{HOMO} of these semiconductors. In Fig. 6, the relaxation time for four different semiconductors, P3HT, PTAA, PTV, and F8T2 is shown as a function of E_{HOMO}. The fact that the time scale of the bias-stress effect decreases with increasing E_{HOMO} is further support for the proton migration mechanism.

General considerations of the electrochemical reactions Eqs. (1) and (2) lead to the expectation that the relaxation time should decrease exponentially with increasing HOMO energy, $\tau \sim \exp(-c E_{HOMO}/k_B T)$. A quantitative prediction of the constant c in this exponential dependence would require detailed information of the electrochemistry taking place in the semiconductor, e.g., information about the coordination shell of a proton. Apart from this, information about the exact amount of water present in the semiconductor in the experiments in Ref. 11 would be needed. In the absence of such information, we can conclude from Fig. 6 that the overall trend is consistent with our model, but that establishing the precise relation between the dynamics of the bias-stress effect and E_{HOMO} is presently beyond our scope.

VIII. SUMMARY, CONCLUSIONS, AND DISCUSSION

We have developed a model for operational instabilities involving threshold voltage shifts in *p*-type organic field-effect transistors with silicon-dioxide as gate dielectric based on a proton migration mechanism. The model is based on the assumption that an equilibrium exists in the accumulation layer of the organic semiconductor between holes and protons because of reactions taking place involving these species and water, and on the assumption that protons can migrate into the oxide, leading to a shielding of the gate electric field.

The model can very accurately describe the bias-stress effect in these transistors, which is manifested as a shift of the threshold voltage toward a constant stressing gate voltage. Because of the large proton density gradient in the oxide, the diffusion contribution of the protons dominates over the drift contribution. In the case that the drift contribution is

neglected, the dependence of the threshold voltage on time follows a universal curve, with a characteristic time as the only parameter. This universal curve is very close to a stretched-exponential function, which explains the success of the description of the shift of the threshold voltage with time in terms of such a function. The model explains the role of water and the observation that the activation energy of the bias-stress effect is virtually independent of the organic semiconductor. The magnitude of the activation energy agrees with a calculated value for transport of protons in the silicon dioxide.

A unique feature of the model is that upon application of a dynamic gate bias it predicts that a situation can occur where the transistor current shows an anomalous non-monotonic temporal behavior. In such a situation, protons temporarily diffuse back from the oxide into the semiconductor, where they are converted back into holes. This can occur while the transistor is continuously in accumulation and hence under stressing conditions. The experimental verification of this prediction is strong support for the validity of the model. We do not know of any other model for the bias-stress effect that can explain such a behavior. The measured anomalous current transients can be accurately described with the model.

The recovery of a transistor that has been exposed to bias stress can also be described with the model. In recovery, protons that have migrated into the oxide during stressing diffuse back to the semiconductor, where they are converted back into holes that are carried away by the source and drain electrodes. This leads to a shift of the threshold voltage back to its original value. The model predicts that the extent of stressing has a large influence on the dynamics of the recovery. A transistor that has been almost fully stressed recovers relatively much slower than a transistor that has been only partially stressed. Therefore, the recovery curves for the threshold-voltage shift cannot be described by a single stretched-exponential function. The measured time dependence of the threshold voltage during recovery quite accurately follows the model predictions, obtained using parameters from the modeling of the threshold-voltage shift for stress. These results have an important technological implication for the operation of organic transistors: an optimal operational time can be obtained by alternating short periods of operation with short periods of recovery.

A prediction of the proton migration mechanism is that with an increasing energy of the HOMO of the organic semiconductor the bias-stress effect should accelerate. This occurs because with increasing HOMO energy the equilibrium between holes and protons existing in the accumulation layer shifts toward a larger proton-hole ratio. The predicted trend was verified for a number of polymeric semiconductors.

Despite the fact that the indications for the validity of the proton migration mechanism in these transistors are extremely strong, a definite proof for the mechanism is still missing. Direct demonstration of the electrolysis of water occurring in these transistors would provide definite proof. However, the predicted amounts of molecular oxygen and hydrogen produced in our experimental setup are extremely small. In fact, they are negligible in comparison to the natural abundances of these gases in ambient air. Exposure to heavy water and demonstration of the presence of deuterium gas, like in Ref. 23, after stress and recovery of a transistor would provide definite proof.

ACKNOWLEDGMENTS

*Author to whom correspondence should be addressed; a.sharma@tue.nl

[1] H. Sirringhaus, Adv. Mater. **17**, 2411 (2005).

[2] L. Zhou, A. Wanga, S. Wu, J. Sun, S. Park, and T. N. Jackson, Appl. Phys. Lett. **88**, 083502 (2006).

[3] R. A. Street, Adv. Mater. **21**, 2007 (2009).

[4] H. Sirringhaus, Adv. Mater. **21**, 3859 (2009).

[5] R. A. Street, A. Salleo, and M. L. Chabinyc, Phys. Rev. B **68**, 085316 (2003).

[6] H. L. Gomes, P. Stallinga, F. Dinelli, M. Murgia, F. Biscarini, and D. de Leeuw, Appl. Phys. Lett. **84**, 3184 (2004).

[7] A. Salleo, F. Endicott, and R. A. Street, Appl. Phys. Lett. **86**, 263505 (2005).

[8] R. A. Street, M. L. Chabinyc, and F. Endicott, J. Appl. Phys. **100**, 114518 (2006).

[9] C. Goldmann, D. J. Gundlach, and B. Batlogg, Appl. Phys. Lett. **88**, 063501 (2006).

[10] M. Debucquoy, S. Verlaak, S. Steudel, K. Myny, J. Genoe, and P. Heremans, Appl. Phys. Lett. **91**, 103508 (2007).

[11] S. G. J. Mathijssen, M. Cölle, H. Gomes, E. C. P. Smits, B. de Boer, I. McCulloch, P. A. Bobbert, and D. M. de Leeuw, Adv. Mater. **19**, 2785 (2007).

[12] M. F. Calhoun, C. Hsieh, and V. Podzorov, Phys. Rev. Lett. **98**, 096402 (2007).

[13] S. G. J. Mathijssen, M. Kemerink, A. Sharma, M. Cölle, P. A. Bobbert, R. A. J. Janssen, and D. M. de Leeuw, Adv. Mater. **20**, 975 (2008).

[14] A. Sharma, S. G. J. Mathijssen, M. Kemerink, D. M. de Leeuw, and P. A. Bobbert, Appl. Phys. Lett. **95**, 253305 (2009).

[15] S. J. Zilker, C. Detcheverry, E. Cantatore, and D. M. de Leeuw, Appl. Phys. Lett. **79**, 1124 (2001).

[16] R. S. Crandall, Phys. Rev. B **43**, 4057 (1991).

[17] J. B. Chang and V. Subramanian, Appl. Phys. Lett. **88**, 233513 (2006).

[18] M. Tello, M. Chiesa, C. M. Duffy, and H. Sirringhaus, Adv. Funct. Mater. **18**, 3907 (2008).

[19] G. Paasch, J. Electroanal. Chem. **600**, 131 (2007).

[20] M. Matters, D. M. de Leeuw, P. Herwig, and A. Brown, Synth. Met. **102**, 998 (1999).

[21] W. Kalb, T. Mathis, S. Haas, A. Stassen, and B. Batlogg, Appl.

Phys. Lett. **90**, 092104 (2007).

[22] A. Sharma, S. G. J. Mathijssen, T. Cramer, M. Kemerink, D. M. de Leeuw, and P. A. Bobbert, Appl. Phys. Lett. **96**, 103306 (2010).

[23] A. Soffer and M. Folman, Trans. Faraday Soc. **62**, 3559 (1966).

[24] J. H. Anderson and P. A. Parks, J. Phys. Chem. **72**, 3662 (1968).

[25] B. C. Senn, P. J. Pigram, and J. Liesegang, Surf. Interface Anal. **27**, 835 (1999).

[26] L. Tsetseris, X. Zhou, D. M. Fleetwood, R. D. Schrimpf, and S. T. Pantelides, MRS Symposia Proceeding No. 786 (Materials Research Society, Pittsburgh, 2004), p. 171.

[27] K. Vanheusden, W. L. Warren, R. A. B. Devine, D. M. Fleetwood, J. R. Schwank, M. R. Shaneyfelt, P. S. Winkour, and Z. J. Lemnios, Nature (London) **386**, 587 (1997).

[28] N. F. M. Devine, J. Robertson, V. Girault, and R. A. B. Devine, Phys. Rev. B **61**, 15565 (2000).

[29] R. A. B. Devine and G. V. Herrera, Phys. Rev. B **63**, 233406 (2001).

[30] J. Godet and A. Pasquarello, Phys. Rev. Lett. **97**, 155901 (2006).

[31] G. T. Yu and S. K. Sen, Appl. Surf. Sci. **202**, 68 (2002).